

## Characterization of $\text{Ge}_{1-x-y}\text{Si}_x\text{Sn}_y$ Ternary Alloy Surfaces and $\text{Ni}/\text{Ge}_{1-x-y}\text{Si}_x\text{Sn}_y$ Bilayer Reactions by X-Ray Techniques

Gordon J. Grzybowski<sup>1,2</sup>, Arnold Kiefer<sup>1</sup>, Bruce Claflin<sup>1</sup>

<sup>1</sup>Air Force Research Laboratory, Sensors Directorate, Wright–Patterson AFB, OH 45433, U.S.A.

<sup>2</sup>Solid State Scientific Corporation, Hollis, NH 03049, U.S.A.

### ABSTRACT

Interest in next generation devices that integrate photonic and electronic functionality is focused on extending the capability of existing group IV material systems while maintaining compatibility with existing processing methods and procedures. One such class of materials which has been recently developed,  $\text{Ge}_{1-x-y}\text{Si}_x\text{Sn}_y$  ternary alloys, is being investigated for integrated Si photonics, solar cell materials, telecommunication applications, and for IR photodetectors. These alloys afford the opportunity to decouple the band gap energies and lattice constants over a wide range of values, potentially yielding direct and indirect character that can be coupled with a variety of different substrates dependent on composition.

In the present work, we report X-ray photoelectron spectroscopy (XPS) characterization of  $\text{Ge}_{1-x-y}\text{Si}_x\text{Sn}_y$  alloys grown by gas-source molecular beam epitaxy (GS-MBE) and investigate  $\text{Ni}/\text{Ge}_{1-x-y}\text{Si}_x\text{Sn}_y$  bilayer reactions with x-ray diffraction (XRD). The surface oxidation of samples stored in ambient conditions were measured with XPS. High resolution spectra showed chemical shifts of Ge, Si and Sn peaks consistent with Ge-O, Si-O and Sn-O bond formation. Depth profiling indicates a homogeneous composition throughout the bulk of the sample with surface oxidation confined to the top few nanometers. A highly tin-enriched layer was indicated at the surface of the material, while silicon was observed to be either enriched or depleted at the surface depending on the sample.

To study the interaction of the ternary with an ohmic contact commonly used in device fabrication processes today, nickel layers 30 nm thick were evaporated onto the alloys and were annealed in nitrogen up to 400 °C for periods as long as 1 hour. The XRD data show that the  $\text{Ni}_2(\text{Ge}_{1-x-y}\text{Si}_x\text{Sn}_y)$  phase forms first followed by  $\text{Ni}(\text{Ge}_{1-x-y}\text{Si}_x\text{Sn}_y)$ .

### INTRODUCTION

Recently, a new material system has emerged as a potential candidate for various electronic and optical applications. The ternary alloy system comprised of Ge, Si, and Sn ( $\text{Ge}_{1-x-y}\text{Si}_x\text{Sn}_y$ ) is able, in principle, to span a wide range of electronic and structural properties including a fundamental direct gap and lattice constants ranging from silicon to tin. [1-4] The system also affords the opportunity to decouple the band gap and lattice parameter [5] which may allow a wide variety of materials to be grown epitaxially with great potential for strain engineering and buffers [6]. Potential applications for these materials include novel on-chip components via integration with Si photonics, multi-junction solar cells, telecom, and infrared sensing [7-9].

The recent emergence of these materials and growth methods means much work still remains in the electronic and structural characterization of this ternary alloy through the range of compositions available. To conduct such studies, electrical contact materials and processing required to produce test devices must be developed. Of particular concern for contact formation

to alloys with high Sn content is preventing Sn precipitation because the equilibrium solubility of Sn in Si and Ge is very low.

A promising contact material is Ni, which has been reported to form a low resistivity ohmic contact on Ge when annealed at low temperatures (300-500 °C), perhaps low enough to prevent Sn precipitation. The Ni<sub>2</sub>Ge phase forms initially followed by NiGe.[10-12] The formation temperature of the low resistivity phase would seem ideal for contact formation with Ge<sub>1-x-y</sub>Si<sub>x</sub>Sn<sub>y</sub> alloys. However, no studies of interactions between Ni contacts and Ge<sub>1-x-y</sub>Si<sub>x</sub>Sn<sub>y</sub> alloys have been conducted.

The formation of good contacts to a material is sensitive to the composition and oxidation of the material surface. In this work we investigate the surface oxidation of Ge<sub>1-x-y</sub>Si<sub>x</sub>Sn<sub>y</sub> alloys on 6° miscut Ge(100) stored in an ambient environment before and after treatment etching with 5% HF/DI water. We also study the interaction of Ni with Ge<sub>1-x-y</sub>Si<sub>x</sub>Sn<sub>y</sub> alloys grown by GS-MBE and annealed at temperatures ranging from 200 °C to 400 °C.

## EXPERIMENT

Alloys with Ge compositions of 85-90%, Si from 8-12%, and Sn 1.9-3 % were grown with GS-MBE. Details of the growth process have been previously reported [13,14]. Thin layers of Ni (30nm) were evaporated onto 900 nm thick Ge<sub>0.85</sub>Si<sub>0.12</sub>Sn<sub>0.03</sub> after etching with buffered HF. The Ni films were then annealed in a tube furnace under flowing nitrogen at temperatures up to 400 °C for up to an hour. A sample of the same composition with no Ni deposited was cleaned in 5% HF/DI water and rinsed with DI water and isopropyl alcohol baths. It was immediately inserted into the XPS to investigate the effectiveness of wet etching to remove surface oxidation.

XPS spectra were collected using a PHI (Perkin Elmer) 5500 spectrometer equipped with a hemispherical analyzer using an Al K<sub>α</sub> x-ray source operated at 350 W. Depth profiles were measured using a rastered 5 kV argon ion sputter beam. Atomic concentrations were determined from integrated core-level XPS peaks of high resolution spectra using known sensitivity factors [15].

X-ray diffraction measurements were performed using a PANalytical Empyrean multipurpose x-ray diffractometer with Cu source, and x-ray mirror incident beam optic. Grazing angle of the incident (3°) beam 2θ-scans with parallel plate collimator, Ni-β filter, and proportional detector were used to collect the spectra. Measurements were taken with a low incident angle (3°) to maximize the sampled volume.

## RESULTS and DISCUSSION

### XPS Surface Analysis

A representative XPS survey spectrum highlights the spectral features used in the quantitative analysis (Fig. 1). High resolution spectra of Ge 2p<sub>3/2</sub>, Sn 3d<sub>5/2</sub>, and Si 2p<sub>3/2</sub> peaks at the surface of Ge<sub>1-x-y</sub>Si<sub>x</sub>Sn<sub>y</sub> alloys maintained in an ambient atmosphere show that all species are oxidized at the surface; however, the oxide layer only persists for a few nanometers as evidenced by the presence of the vanishing O 1s peak, and the chemical shifts of Ge, Si and Sn peaks from higher to lower binding energies.

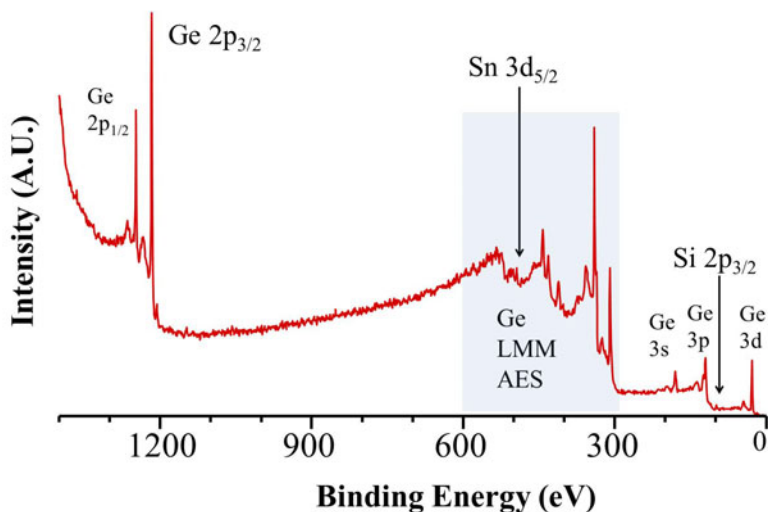


**Figure 1.** Representative XPS spectra of  $\text{Ge}_{1-x-y}\text{Si}_x\text{Sn}_y$  alloy with high germanium content. It shows the qualitative position and intensity of the peaks used in analysis.

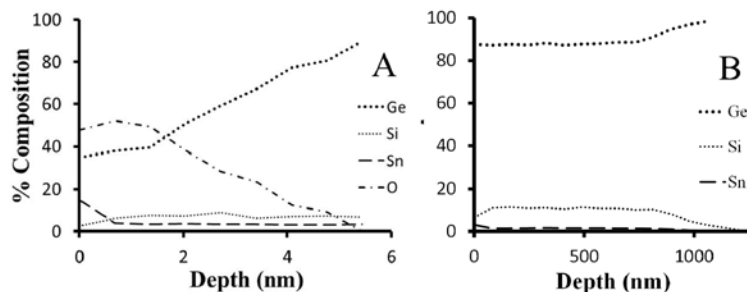


**Figure 2.** The surface (A) and bulk (B) composition profile of a  $\text{Ge}_{0.88}\text{Si}_{0.11}\text{Sn}_{0.01}$  alloy measured by XPS. These bulk values are consistent with the film composition  $\text{Ge}_{0.85}\text{Si}_{0.12}\text{Sn}_{0.03}$  determined by RBS.

Figure 2a shows an XPS depth profile of the composition in the surface region (top 6 nm) of a  $\text{Ge}_{0.85}\text{Si}_{0.12}\text{Sn}_{0.03}$  sample compared with the composition through the entire film thickness (Fig. 2b). The oxygen content quickly decreases after 1.5 nm and is eliminated by 6 nm while the Ge concentration increases from 30% to 90%. Interestingly, the Si concentration is depleted to 2.5% and quickly increases to a steady 7-8% within the surface region. Sn shows the opposite

effect; it is greatly enhanced (near 15%) at the surface but quickly reduces to the bulk value of 3%. This Sn enhancement has been observed in all samples under study and has been as high as 25% for some material. Silicon was observed to be either depleted or enriched at the surface depending on the sample. Analysis of the depth profile data from the bulk material beyond 6 nm, indicates a homogeneous composition throughout. The average composition was calculated to be  $\text{Ge}_{0.88}\text{Si}_{0.11}\text{Sn}_{0.01}$ . The data is consistent with the composition determined by RBS that indicates a composition of  $\text{Ge}_{0.85}\text{Si}_{0.12}\text{Sn}_{0.03}$ .

As noted above, surface Ge, Si, and Sn species were oxidized. To determine a process for removing the oxide from the surface prior to metals deposition, a sample of the material was dipped in 5% HF/DI water for 2 minutes and rinsed in DI water and isopropanol. XPS spectra were taken before and after cleaning and indicated the surface oxide was eliminated. The XPS spectra show a chemical shift of Ge, Sn, and Si peaks to higher binding energies before the cleaning as is characteristic of oxidized species (Figure 3). After etching all oxide has been removed.

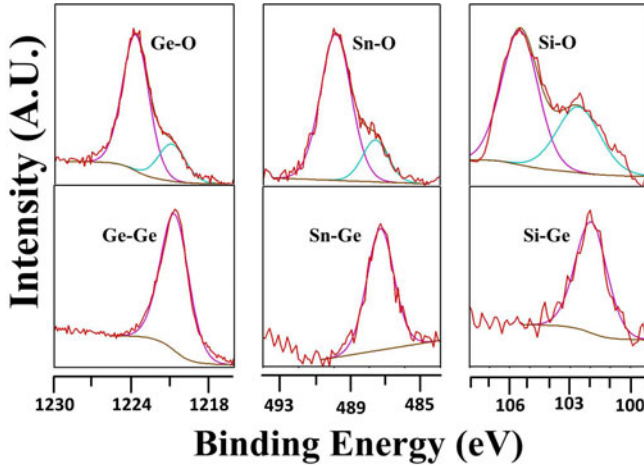


**Figure 3.** Spectrum of  $\text{Ge}2\text{P}_{3/2}$ ,  $\text{Sn}3\text{d}_{5/2}$ , and  $\text{Si}2\text{P}_{3/2}$  peaks before (top) and after (bottom) HF etching. The data shows removal of all surface oxide species.

#### **XRD analysis of Ni-GeSiSn interaction**

Reactions of Ni and Ge are known to produce Ni rich phases ultimately leading to NiGe under constant temperature ramp and isothermal conditions.[10-12] In this work an alloy with composition  $\text{Ge}_{0.85}\text{Si}_{0.12}\text{Sn}_{0.03}$  was reacted with Ni layers by annealing at temperatures up to 400 °C for times up to 1 hour. The alloy is lattice matched to Ge using the 4:1 ratio of Si and Sn respectively. Representative diffraction patterns are shown in Figure 4.

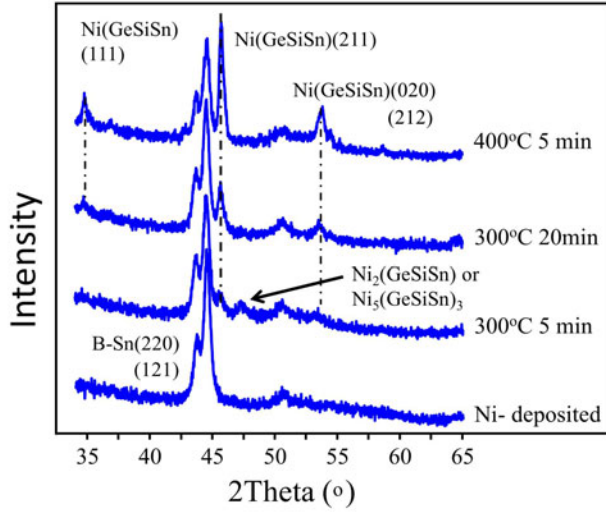


**Figure 4.** XRD scans at a fixed grazing incidence ( $3^\circ$ ) of a  $\text{Ge}_{0.85}\text{Si}_{0.12}\text{Sn}_{0.03}$  alloy with Ni contacts subjected to different anneals. Orthorhombic  $\text{Ni}_2(\text{Ge}_{0.85}\text{Si}_{0.12}\text{Sn}_{0.03})$  or monoclinic  $\text{Ni}_3(\text{Ge}_{0.85}\text{Si}_{0.12}\text{Sn}_{0.03})_3$  forms during a 5 minute anneal at  $300^\circ\text{C}$  while continued annealing at this temperature or higher forms  $\text{Ni}(\text{Ge}_{0.85}\text{Si}_{0.12}\text{Sn}_{0.03})$ .

For short anneals at  $300^\circ\text{C}$ ,  $\text{Ni}(\text{Ge}_{0.85}\text{Si}_{0.12}\text{Sn}_{0.03})$  was observed to form with  $\text{Ni}_2(\text{Ge}_{0.85}\text{Si}_{0.12}\text{Sn}_{0.03})$  or  $\text{Ni}_3(\text{Ge}_{0.85}\text{Si}_{0.12}\text{Sn}_{0.03})_3$  quickly followed by elimination of the Ni-rich phase as temperature or time increases. The peaks corresponding to the  $\text{Ni}(\text{Ge}_{0.85}\text{Si}_{0.12}\text{Sn}_{0.03})$  alloy are found at  $2\theta$  positions  $34.7^\circ$ ,  $36.7^\circ$ ,  $45.6^\circ$ , and  $53.6^\circ$ , and can be best seen for the sample annealed at  $400^\circ\text{C}$  in Fig. 4. The peaks are assigned based on the expected structural similarity of the quaternary alloy to NiGe. The Bragg peaks for the (1 1 1), (2 1 1), (0 2 0) and (2 1 2), and (1 0 2) planers of NiGe at  $2\theta$  angles of  $34.6^\circ$ ,  $36.7^\circ$ ,  $45.6^\circ$ , and  $53.4^\circ$  [16]. Some evidence for texturing was found in symmetric scans of material annealed for an hour at  $400^\circ\text{C}$  which only showed the (1 1 1) peak.

Only observed in anneals at low temperature and short time, the peak at  $47.3^\circ$  is consistent with  $\text{Ni}_2(\text{Ge}_{0.85}\text{Si}_{0.12}\text{Sn}_{0.03})$  (0 2 0) or (1 1 3) which are found at  $47.4^\circ$  and  $47.8^\circ$  respectively in  $\text{Ni}_2\text{Ge}$ . [17] However, the most intense peak in  $\text{Ni}_3\text{Ge}_3$  (3 3 1) is found at  $46.7^\circ$ , and given the uncertainty in strain state and microstructure  $\text{Ni}_3(\text{Ge}_{0.85}\text{Si}_{0.12}\text{Sn}_{0.03})_3$  cannot be ruled out either [17]. Adding to the difficulty assigning this peak is that the most intense peaks in  $\text{Ni}_2\text{Ge}$  overlap with peaks from  $\beta\text{-Sn}$  which also overlap with the most intense peak in Ni. Additionally, the presence of substrate effects at  $51^\circ$  and the absence of the Ni (0 0 2) peak, expected at  $51.9^\circ$ , appear in the spectra, but do not affect the analysis.

Due to the Ge lattice matched composition of the alloy, the diffraction data is consistent with both substitutional Sn and Si on Ge lattice sites of NiGe, and also with NiGe phase segregation. While there is no evidence for binary Ni-Sn and Ni-Si compounds in the diffraction data, phase segregation of Ge cannot be ruled out.

## CONCLUSIONS

We used XPS to show that the surface of GeSiSn alloys can have vastly different compositions than the bulk material, and that each species is oxidized in an ambient environment. The surface oxide extends for the first 6 nm and can be removed completely by etching in dilute HF. We have also shown using XRD that bilayer reactions of Ni and  $\text{Ge}_{1-x-y}\text{Si}_x\text{Sn}_y$  alloys at temperatures as low as 300 °C are consistent with pseudomorphic NiGe. The alloy forms through  $\text{Ni}_3(\text{Ge}_{1-x-y}\text{Si}_x\text{Sn}_y)_3$  or  $\text{Ni}_2(\text{Ge}_{1-x-y}\text{Si}_x\text{Sn}_y)$  and ultimately leads to  $\text{Ni}(\text{Ge}_{1-x-y}\text{Si}_x\text{Sn}_y)$  with longer annealing times or higher temperatures. The low temperature formation indicates a good candidate for ohmic contact formation with  $\text{Ge}_{1-x-y}\text{Si}_x\text{Sn}_y$  alloys with high Sn contents.

## ACKNOWLEDGMENTS

The authors would like to thank Prof. J. Kouvetakis and Prof. J. Menendez for providing samples under AFRL contract #FA8650-13-C-1535 (B. Clafin) and for helpful discussions. This work was supported by AFOSR LRIR 13RY05COR (G. Pomrenke).

## REFERENCES

1. V. R. D'Costa, Y.-Y. Fang, J. Tolle, J. Kouvetakis, and J. Menendez, *Phys. Rev. Lett.* **102**, 107403 (2009).
2. D. W. Jenkins and J. D. Dow, *Phys. Rev. B* **36**, 7994 (1987).
3. P. Moontragoon, R. A. Soref and Z. Ikonc, *J. Appl. Phys.* **112**, 073106 (2012).
4. J. D. Gallagher, C. Xu, L. Jiang, J. Kouvetakis, and J. Menendez, *Appl. Phys. Lett.* **103**, 202104 (2013).
5. J. Kouvetakis, J. Menendez, A.V. G. Chizmeshya, *Annu. Rev. Mater. Res.* **36**, 497 (2006)
6. R. Soref, *Nat. Photonics* **4**, 495 (2010).
7. Y.-Y. Fang, J. Xie, J. Tolle, R. Roucka, V. R. D'Costa, A. V. G. Chizmeshya, J. Menendez, and J. Kouvetakis, *J. Am. Chem. Soc.* **130**, 16095 (2008).
8. G. Sun, R. A. Soref, and H. H. Cheng, *J. Appl. Phys.* **108**, 033107 (2010).
9. G. Sun, H. H. Cheng, J. Menendez, J. B. Khurgin, and R. A. Soref, *Appl. Phys. Lett.* **90**, 251105 (2007).
10. L. J. Jin et al., *Thin Solid Films* **151**, 462 (2004)
11. E. D. Marshall, C.S. Wu, C.S. Pai, M.S. Scott, S. S. Lau, *Mater. Res. Society symp. Proc.* **47**, 161 (1985)
12. S. Gaudet, C. Datavernier, C. Lavoie, P. Desjardins, *J. Appl. Phys.* **100**, 034306 (2006)
13. H. Lin, R. Chen, W. Lu, Y. Huo, T. I. Kamins, and J. S. Harris, *Appl. Phys. Lett.* **100**, 141908 (2012).
14. G. H. Wang, E.-H. Toh, X. Wang, S. Tripathy, T. Osipowicz, T. K. Chan, K.-M. Hoe, S. Balakumar, G.-Q. Lo, G. Samudra, and Y.-C. Yeo, *Appl. Phys. Lett.* **91**, 202105 (2007)
15. J. F. Moulder et al., *Handbook of X-Ray Photoelectron Spectroscopy*, Perkin-Elmer Corporation, Eden Prairie, MN (1992).
16. K. Schubert, H. Pfisterer, *Zeitschrift fuer Metallkunde*, **41**, 358 - 367, (1950)
17. K. Schubert, T. Goedecke, M. Ellner, *Journal of the Less-Common Metals*, **24**, 23-40, (1971)